Deep-Sea Research II 58 (2011) 2695–2706

Contents lists available at ScienceDirect

Deep-Sea Research II

journal homepage: www.elsevier.com/locate/dsr2

Observation of consistent trends in the organic complexation of dissolved iron in the Atlantic sector of the Southern Ocean

C.-E. Thuróczy [a,*], L.J.A. Gerringa [a], M.B. Klunder [a], P. Laan [a], H.J.W. de Baar [a,b]

[a] Royal Netherlands Institute for Sea Research (Royal NIOZ), P.O. Box 59, 1790 AB Den Burg, Texel, The Netherlands
[b] Department of Ocean Ecosystems, University of Groningen, Groningen, The Netherlands

ARTICLE INFO

Article history:
Received 21 January 2011
Accepted 21 January 2011
Available online 27 January 2011

Keywords:
Iron
Organic complexation
Ligands
Ratio ligand/iron
Southern Ocean
CLE-AdSV
GEOTRACES

ABSTRACT

Organic complexation of dissolved iron (dFe) was investigated in the Atlantic sector of the Southern Ocean in order to understand the distribution of Fe over the whole water column. The total concentration of dissolved organic ligands ([Lt]) measured by voltammetry ranged between 0.54 and 1.84 nEq of M Fe whereas the conditional binding strength (K') ranged between $10^{21.4}$ and $10^{22.8}$. For the first time, trends in Fe–organic complexation were observed in an ocean basin by examining the ratio ([Lt]/[dFe]), defined as the organic ligand concentration divided by the dissolved Fe concentration. The [Lt]/[dFe] ratio indicates the saturation state of the natural ligands with Fe; a ratio near 1 means saturation of the ligands leading to precipitation of Fe. Reversely, high ratios mean Fe depletion and show a high potential for Fe solubilisation. In surface waters where phytoplankton is present low dissolved Fe and high variable ligand concentrations were found. Here the [Lt]/[dFe] ratio was on average 4.4. It was especially high (5.6–26.7) in the HNLC (High Nutrient, Low Chlorophyll) regions, where Fe was depleted. The [Lt]/[dFe] ratio decreased with depth due to increasing dissolved Fe concentrations and became constant below 450 m, indicating a steady state between ligand and Fe. Relatively low [Lt]/[dFe] ratios (between 1.1 and 2.7) existed in deep water north of the Southern Boundary, facilitating Fe precipitation. The [Lt]/[dFe] ratio increased southwards from the Southern Boundary on the Zero Meridian and from east to west in the Weddell Gyre due to changes both in ligand characteristics and in dissolved iron concentration.

High [Lt]/[dFe] ratio expresses Fe depletion versus ligand production in the surface. The decrease with depth reflects the increase of [dFe] which favours scavenging and (co-) precipitation, whereas a horizontal increase in the deep waters results from an increasing distance from Fe sources. This increase in the [Lt]/[dFe] ratio at depth shows the very resistant nature of the dissolved organic ligands.

1. Introduction

The presence and availability of iron (Fe) is vital for life in the ocean. This trace nutrient is used by most organisms in seawater including phytoplankton in the euphotic zone. Phytoplankton is not only the base of the food web; it is also largely responsible for the fixation of dissolved carbon dioxide and the production of dissolved oxygen. Iron is used in phytoplankton cells in different locations and processes (Sunda et al., 1991; Sunda, 2001), notably in photosynthesis (photosystems) and in enzymes (e.g. nitrate-reductase). Due to its low concentration in seawater, iron is a limiting factor of primary production (Martin and Gordon, 1988; Martin et al., 1991; de Baar et al., 1990, 1995; Buma et al., 1991; Coale et al., 1996; Fitzwater et al., 1996; Timmermans et al., 1998, 2001, 2004) especially in HNLC (high nutrient, low chlorophyll, Martin et al., 1991) regions such as those in the Southern Ocean. Iron is used in the surface by phytoplankton but also over the whole water column by microbial communities (Bacteria and Archaea) (Tortell et al., 1996, 1999) responsible for the degradation and remineralisation of sinking organic matter. Iron is found in seawater at concentrations above those determined by the solubility product (Kuma et al., 1996; Millero, 1998). This is due to Fe-binding organic ligands. Indeed 95–99.9% of the dissolved Fe is strongly complexed by natural organic ligands (Gledhill and van den Berg, 1994; Rue and Bruland, 1995; Wu and Luther, 1995; Nolting et al., 1998; Powell and Donat, 2001) allowing Fe to remain in solution, yet possibly limiting its availability for direct biological uptake.

The knowledge of the chemistry of Fe is important to understand its cycle in the world ocean which determines its distribution over the water column. The distribution of Fe in the oceans is controlled by its sources (aerosols deposition to the surface ocean, upwelling, ice melting and hydrothermal events), and by competition between

* Corresponding author. Tel.: +31 222 369 436.
E-mail address: Charles-Edouard.Thuroczy@nioz.nl (C.-E. Thuróczy).

0967-0645/$ - see front matter
doi:10.1016/j.dsr2.2011.01.002

processes which stabilise and remove it. Organic complexation stabilises Fe in seawater by keeping it in solution thus increasing its residence time. Fe removal is mainly caused by precipitation as oxy-hydroxides, adsorption onto large particles or colloid aggregation (Alldredge et al., 1993; Wells and Goldberg, 1993, 1994; Wells et al., 2000; Kepkay, 1994; Logan et al., 1995; Wu et al., 2001; Cullen et al., 2006).

The work presented here forms part of the GEOTRACES programme (www.geotraces.org, GEOTRACES Planning Group, 2006). As part of this programme, the distribution of Fe along the Zero Meridian (Klunder et al., 2011) and several other trace elements, including dissolved aluminium and manganese (Middag et al., 2011), were also investigated.

This study describes the organically complexed state of Fe over the whole water column and the observed changes in the Fe chemistry when passing from the Sub-Antarctic Ocean into the Weddell Gyre (HNLC regions). With the knowledge of the Fe chemistry and of the organically complexed Fe in the whole water column, the processes controlling the Fe distribution in the world oceans can be better understood.

2. Materials and methods

2.1. Cleaning procedures

All sample bottles (Nalgene, low-density polyethylene, LDPE, 60–1000 mL) were treated following a 3 steps cleaning procedure (detergent solution, 6 M HCl and 3 M nitric acid) in hot baths (Middag et al., 2009). Finally, the bottles were stored filled with 0.2 M 3QD-HNO_3 (from 65% reagent grade, J.T. Baker). All rinsing were done with MQ water (Millipore Milli-Q deionised water, $R > 18.2\ M\Omega\ cm^{-1}$).

2.2. Area description and sampling strategy

The ANT XXIV/3 expedition onboard R.V. *Polarstern* started from Cape Town, South Africa (February 2008), going south-westwards and reached the Zero Meridian at ~50°S (Fig. 1). The Sub-Tropical Front (STF), the Sub-Antarctic Front (SAF), the Polar Front (PF) and the Southern boundary of the Antarctic Circumpolar Current (SB in the present study) were successively crossed on the Zero Meridian. The Southern Boundary is also called SBdy in the Drake Passage by others (Barré et al., 2008). The expedition continued across the Weddell Sea to King Georges Island, and finally traversed the Drake Passage until arrival in Punta Arenas, Chile (April 2008).

Overall 10 stations were sampled (Fig. 1), for a total of 82 samples: 7 stations along the Zero Meridian, 2 stations in the Weddell Sea and 1 station in the Drake Passage. Each sample was taken at judiciously chosen depths in order to sample all the different water masses present. The different water masses descriptions are detailed by others (Pollard et al., 2002; Middag et al., 2011; and authors they refer to).

The sampling system used was the ultraclean Titan Mk.II permitting metal clean sampling (de Baar et al., 2008). Filtration (0.2 µm pore size, Sartorius Sartobran-300) was done directly in clean-air container: "In fact this is within the more stringent criteria of an ISO Class 6 clean room (formerly US FED STD 209E Class 1000)", in de Baar et al. (2008). Samples for Fe speciation were stored at 0 °C when their analysis could be performed within 2 days; otherwise they were immediately frozen at −20 °C in the dark.

2.3. Brief description of the temperature, salinity, nutrients and fluorescence

Temperature and salinity (conductivity) were measured directly from 2 CTD systems (Sea Bird electronics, regularly calibrated using

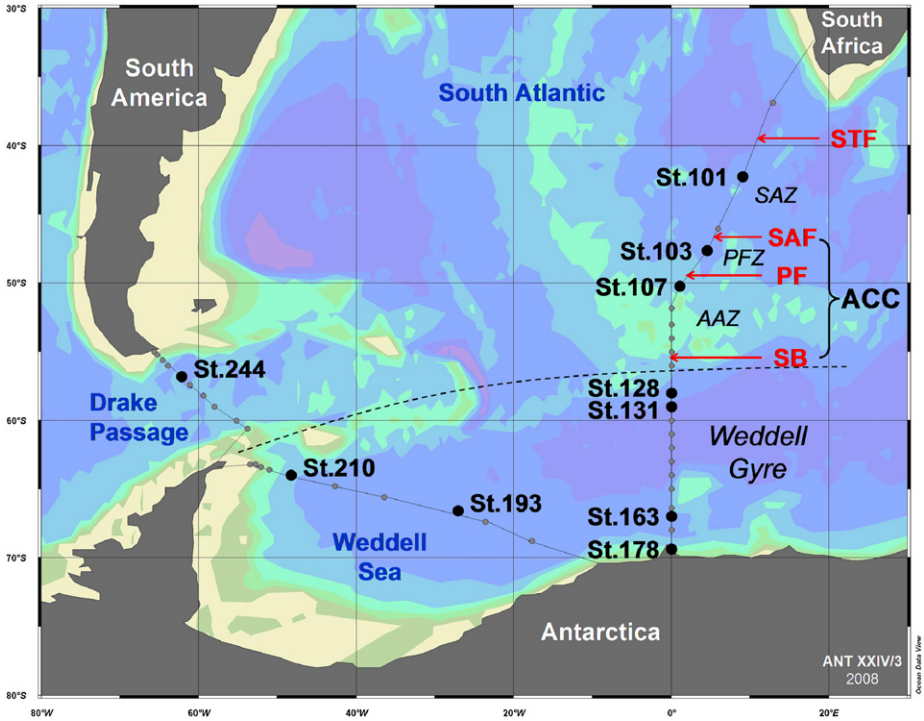

Fig. 1. Chart of the Atlantic sector of the Southern Ocean and location of the fronts and zones. The 10 stations sampled for this study are indicated by large black dots with station numbers. The small grey dots represent the additional stations also sampled with the titanium frame from NIOZ. The dashed line delimits the Weddell Gyre. STF=Sub-Tropical Front; SAF=Sub-Antarctic Front; PF=Polar Front; SB=Southern Boundary; SAZ=Sub-Antarctic Zone (St. 101); PFZ=Polar Frontal Zone (St. 103); AAZ=Antarctic Zone (St. 107); ACC=Antarctic Circumpolar Current; Weddell Gyre (St. 128, 131, 163, 178, 193 and 210).

salinity samples) on the sampling frames (a normal rosette from Alfred-Wegener-Institute and the titanium frame from NIOZ).

The temperature range varied between locations and depths from more than 10 °C in surface layer of the first northernmost station to seawater freezing point (−1.85 °C) in the surface layer in the Weddell Sea and close to the ice edge. This drop in temperature went stepwise through the frontal zones (described by Pollard et al., 2002).

Salinity increased towards the bottom (from approximately 33.7 to 34.1 in the surface to 34.6 to 34.8 at the bottom) with a well defined halocline. This halocline (above 250 m) was stronger in the Weddell Gyre (St. 128, 131, 163, 193 and 210) where freshwater was abundant due to ice melting. At the other stations (101, 103, 107 and 244), this gradient was less pronounced.

The inorganic dissolved nutrients nitrate+nitrite (NO_2+NO_3), phosphate (PO_4) and silicate (SiO_4) were measured directly onboard according to the procedure detailed by Grashoff et al. (1983). The distribution surface of nutrients also showed a distinction between the stations situated north of the SB (Sub-Antarctic stations: 101, 103, 107 and 244) with a depletion of nutrients due to phytoplankton uptake; and those located in the Weddell Gyre (HNLC region, stations 128, 131, 163, 178, 193 and 210) with higher concentrations.

Fluorescence, given in arbitrary unit (a.u.), was obtained from the NIOZ CTD sensor installed on the titanium frame. It corresponds to chlorophyll-*a* and is an indicator of phytoplankton biomass in seawater (Kiefer, 1973; Babin et al., 1996). Relatively high values in surface waters corresponding to a chlorophyll maximum at about 50 m depth (euphotic zone) and a decrease with depth towards the aphotic zone were observed. At station 178 the fluorescence could even be detected at ~140 m depth. Table 1 shows the average of fluorescence in the surface layer per station when it was >0.1 a.u. Stations 101 and 103 had relatively high fluorescence compared to stations 131 and 210 where lower fluorescence was recorded. Close to the ice edge (St. 163 and 178) the highest fluorescence of all stations was measured due to a phytoplankton bloom.

2.4. Dissolved iron

Dissolved Fe (<0.2 μm) was measured onboard (Klunder et al., 2011) following the method described by de Jong et al. (1998), with minor modifications (de Baar et al., 2008). The samples used for this study were taken at the same time, from the same GO-FLO samplers and using the same filter cartridge, at a selection of the same stations and casts as those shown by Klunder et al. (2011) but in separate (i.e. duplicate) sample bottles. They were acidified to pH 1.8 using 12 M ultraclean HCl (Baseline® Hydrochloric Acid, Seastar Chemicals Inc.). The samples were left for at least 12 h before analysing. To ensure all Fe was in its oxidised state (Fe(III)), 60 μL of a 1‰ hydrogen peroxide (Merck, Suprapur 30%) solution was added 1 h before measuring (Lohan et al., 2005).

The standard deviation of the dissolved Fe concentration determined was always below 5% considering 3 measurements (Klunder et al., 2011).

Table 1
Averaged fluorescence (arbitrary unit, a.u.) in the surface layer per station. Standard deviations, the number of samples (*n*) and the maximum depth (m) where fluorescence >0.1 a.u. are shown.

Stations	Fluorescence (a.u.)	Std. dev.	*n*	Maximum depth (m)
101	0.41	0.21	6	100
103	0.59	0.26	5	75
107	0.30	0.02	6	100
128	0.27	0.04	5	90
131	0.11	0.01	4	100
163	0.94	0.51	6	100
178	1.01	0.97	7	140
193	0.42	0.17	6	100
210	0.16	0.01	4	50
244	0.24	0.02	7	100

2.5. Dissolved organic ligands

2.5.1. Voltammetric procedure and sample treatment

Organic complexation of Fe was determined by Competing Ligand Exchange–Adsorptive Stripping Voltammetry (CLE-AdSV) using 2-(2-Thiazolylazo)-p-cresol (TAC) as a competing ligand (Croot and Johanson, 2000). The voltammetric equipment consisted of a μAutolab potentiostat (Type II, Ecochemie, The Netherlands) and a mercury drop electrode (model VA 663 from Metrohm). The mercury drop size was approximately 0.25 mm^2. The reference electrode was double-junction, Ag/AgCl, 3 M KCl, with a salt bridge filled with 3 M KCl and a glassy carbon counter-electrode. Samples were stirred with a PTFE Teflon stirrer (3000 rpm). A current filter (Fortress 750, Best Power) on which the equipment was linked was used to prevent electrical noise.

The seawater sample was buffered to pH 8.05 by adding a mixed NH_3/NH_4OH borate buffer (final concentration 5 mM). The buffer stock was 1 M boric acid, (Suprapur, Merck) in 0.25 M ammonia (Suprapur, Merck) cleaned through a SepPak C18 column with 20 μM TAC (2-(2-Thiazolylazo)-p-cresol). A stock of 0.02 M TAC was prepared in 3QD-Methanol for a final concentration of 10 μM in the seawater sample (Croot and Johanson, 2000). Additions of Fe(III) standard (0, 0.33, 0.5, 0.67, 1, 1.5, 2, 2.5, 3, 4, 6, 8 nM) were done with a stock of 1 μM Fe(III) (prepared in 0.03 M HCl, Seastar chemicals Inc.) in a series of 13 Teflon PFA vials (30 mL volume; Savillex 201-030-10-033-01) including 2 blanks. The seawater sample was poured (15 mL) into the Teflon PFA vials and were left overnight to equilibrate before analyses by voltammetry.

Before using the Teflon PFA vials, they were preconditioned twice in two successive days (with equilibration overnight) with the complete mixture of seawater and reagents as described above. The preconditioning of the Teflon PFA vials was necessary if they were not used for 4 days.

Each equilibrated aliquot was poured into the voltammetric Teflon cell and purged with nitrogen for 180 s. The differential pulse method was used. The deposition potential of −0.4 V was applied during 140–200 s (depending on the sample and on the sensitivity of the equipment) and the sample was stirred to allow a better adsorption of the complex $Fe(TAC)_2$ on the mercury drop. An equilibration time of 5 s without stirring was done before scanning between −0.4 and −0.7 V at 1.95 mV s^{-1} (modulation amplitude was 25.05 mV). Modulation time was 0.01 s and interval time was 0.1 s. The visible peak due to the dissociation of the Fe-complex and subsequent reduction of Fe(III) was found between −0.460 and −0.500 V.

2.5.2. Calculation of iron speciation

The ligand characteristics were estimated assuming the presence of only one ligand pool. Ligand concentrations [Lt] (in nano-Equivalent of molar of Fe, nEq of M Fe), conditional stability constants log K' (with natural organic ligands) and their respective standard deviations were calculated using the Langmuir model (Eq. (1), non-linear regression of the Langmuir isotherm, Gledhill and van den Berg, 1994; Gerringa et al., 1995). By using the Langmuir model (Eq. (1)) it is assumed that equilibrium between all Fe(III) species exists, all binding sites between Fe and the

unknown ligand L are equal and that the binding is reversible

$$[FeL] = \frac{K' \times [Fe^{3+}] \times [Lt]}{(1 + K' \times [Fe^{3+}])} \quad (1)$$

where [FeL] is the concentration of the natural Fe–ligand complex and $[Fe^{3+}]$ the ionic Fe concentration. The values of [FeL] and $[Fe^{3+}]$ were calculated following Eqs. (2) and (3), respectively,

$$[FeL] = [dFe] + [Fe_{added}] - [Fe(TAC)_2] \quad (2)$$

with [dFe] as the concentration of dissolved Fe measured (see Section 2.4) and $[Fe_{added}]$ as the added Fe for the titration.

$$\left[Fe^{3+}\right] = \frac{[Fe(TAC)_2]}{\alpha_{Fe(TAC)2}} \quad (3)$$

where the term $[Fe(TAC)_2]$ represents the concentration of the Fe bound to TAC calculated by dividing the peak height (nA) by the slope (S=sensitivity, using usually 6 points) of the straight part of the titration curve. The sensitivity was corrected for the influence of ligand sites not yet saturated, as explained by Turoczy and Sherwood (1997) and Hudson et al. (2003). The correction here was done by an algebraic solution of the equilibrium equations, in which S is determined together with L and K'. The parameters S, L and K' are given with the standard deviation of the fit of the data from the model.

$$\alpha_{Fe(TAC)_2} = \beta_{Fe(TAC)_2} \times [TAC]^2 = 10^{12.4} \quad (4)$$

with [TAC]=10 μM, and with $\beta_{Fe(TAC)_2}$ the conditional stability constant of Fe with TAC assuming an equilibrium as follows (Croot and Johanson, 2000):

$$\beta_{Fe(TAC)_2} = [Fe(TAC)_2]/[Fe^{3+}] \times [TAC]^2 = 10^{22.4} \quad (5)$$

For the calculation of pFe (free Fe(III) concentration), the negative logarithm of $[Fe^{3+}]$, the sum of the measured alpha of the natural organic ligands (product of the concentration of excess L and $K'=[L'] \times K'$) and that of the alpha of the inorganic ligands ($\alpha_{inorg}=10^{10}$ after Millero, 1998) were used as follows:

$$pFe = -\log[Fe^{3+}] = -\log\{[dFe]/(\alpha_{org} + \alpha_{inorg})\} \quad (6)$$

The detection limit of the method was determined as 3 times the standard deviation of several blank measurements and was 0.040 nEq of M Fe (n=11). The chemical blank was below this detection limit.

3. Results

3.1. Dissolved Fe distribution (Fig. 2 and Table 2)

The concentrations of dissolved Fe along the Zero Meridian from the same expedition are shown in detail by Klunder et al. (2011). At the stations presented here, the concentration of dissolved Fe was always below the nano-molar level and showed a nutrient-like vertical profile. With a surface minimum at all stations (between 0.02 and 0.19 nM) the concentration of dissolved Fe increased with depth with a maximum just above the seafloor (St. 163: 0.58 nM and St. 193: 0.59 nM), or became more or less constant below 500–1000 m (St. 101: 0.63 nM; St. 103: 0.56 nM; St. 131: 0.36 nM and St. 244: 0.40 nM). Station 107 located south of the PF showed variability in the concentrations of dissolved Fe in the upper layers (0–450 m). It remained constant below 450 m at ~0.55 nM. At station 128 a steep increase was found from the surface until 450 m (until 0.76 nM) followed by a minimum at 1000 m (0.35 nM), and by a second maximum at 2500 m (0.68 nM) and a decrease towards the bottom. Two samples were taken at station 178 in the upper water at 137 and 451 m depth with 0.08 and 0.17 nM of Fe, respectively. Station 210 close to the Antarctic Peninsula slope had a maximum concentration of Fe between 1000 and 1500 m (0.46 nM) ascribed to hydrothermal input (Klunder et al., 2011).

3.2. Organic ligand distribution and characteristics (Fig. 2 and Tables 2 and 3)

The concentration of ligands throughout the water column ranged between 0.49 and 1.84 nEq of M Fe (nano-Equivalents of molar Fe). The upper 450 m showed relatively variable ligand concentrations. At stations 101, 131, 163 and 193 the concentrations were between 0.5 and 1.2 nEq of M Fe in the first 450 m. At stations 103, 107, 128 and 210 a maximum (1.1–1.9 nEq of M Fe) was observed between 70 and 310 m depth after a surface minimum (0.5–0.9 nEq of M Fe).

Below 450 m depth the concentration of ligand decreased towards the bottom at station 101, 107 and 128. The ligand concentration was relatively constant at station 163. Station 131 showed higher concentrations of ligand near the seafloor (around 1.09 nEq of M Fe). The concentration of ligand increased gradually towards the seafloor in the Weddell Sea at stations 193 and 210. At station 244, the concentration of ligand was stable from the surface until 3500 m around 1.33 nEq of M Fe. Near the seafloor it was about 1.00 nEq of M Fe.

The concentration of excess ligand (Excess L=L') with respect to Fe([Lt]−[dFe], Table 2) corresponds to the concentration of free Fe-binding sites. A small value of excess L means a near saturation of the ligand. In the upper layer (0–450 m) the mean values of excess L were 0.62 nEq of M Fe north of the SB, 0.79 nEq of M Fe in the Weddell Gyre on the Zero Meridian, 0.85 nEq of M Fe in the Weddell Sea and 1.27 nEq of M Fe in the Drake Passage (Table 3). Below 450 m depth, the averaged concentrations of excess L were 0.47, 0.56, 0.86 and 0.94, respectively, for the same zones. A surface maximum in excess L was usually found (St. 101, 107, 131, 163, 193 and 244). This excess L increased in average southwards the Southern Boundary on the Zero Meridian. More excess L was found close to the Antarctic ice edge as well as in the Weddell Sea and in the Drake Passage.

The binding strength is defined by the conditional stability constant K' (Table 2). The K' ranged between $10^{21.45}$ and $10^{22.94}$. The value of K' was variable in the first 500–1000 m in all stations and it slightly increased with depth on the Zero Meridian. At station 193 in the Weddell Sea, K' was also variable with high values of K' at 750 m depth ($10^{22.82}$) and at 3000 m depth ($10^{22.76}$). At station 210, K' was constant over the water column, except at the surface and at 1000 m where higher values were found. In the Drake Passage, the value of K' was constant ($10^{22.15}$) over the water column except for the shallowest and deepest samples.

The organic alpha was relatively constant (about 10^{13}) from 450 m depth towards the bottom at all stations. Variable values of organic alpha were found in the first 450 m layer, ranging from 10^{12} at station 101 to $10^{13.5}$ at station 244. Below 450 m depth at the stations north of the SB and in the north part of the Weddell Gyre (until station 131) the values of organic alpha were smaller than 10^{13}. Below 450 m depth at the stations close to the Antarctic ice edge, in the Weddell Sea and in the Drake Passage the values of organic alpha were larger than 10^{13} due to higher excess L in these regions.

Relatively low pFe values (Table 2) corresponding to relatively high free Fe concentrations are due to lower organic alpha values and thus either weaker ligands or lower concentrations of excess L. At stations 101 until 131, pFe decreased from 22.5–23 at the surface to approximately 22 at 450 m depth and remained constant towards the bottom. At stations 163, 193, 210 and 244,

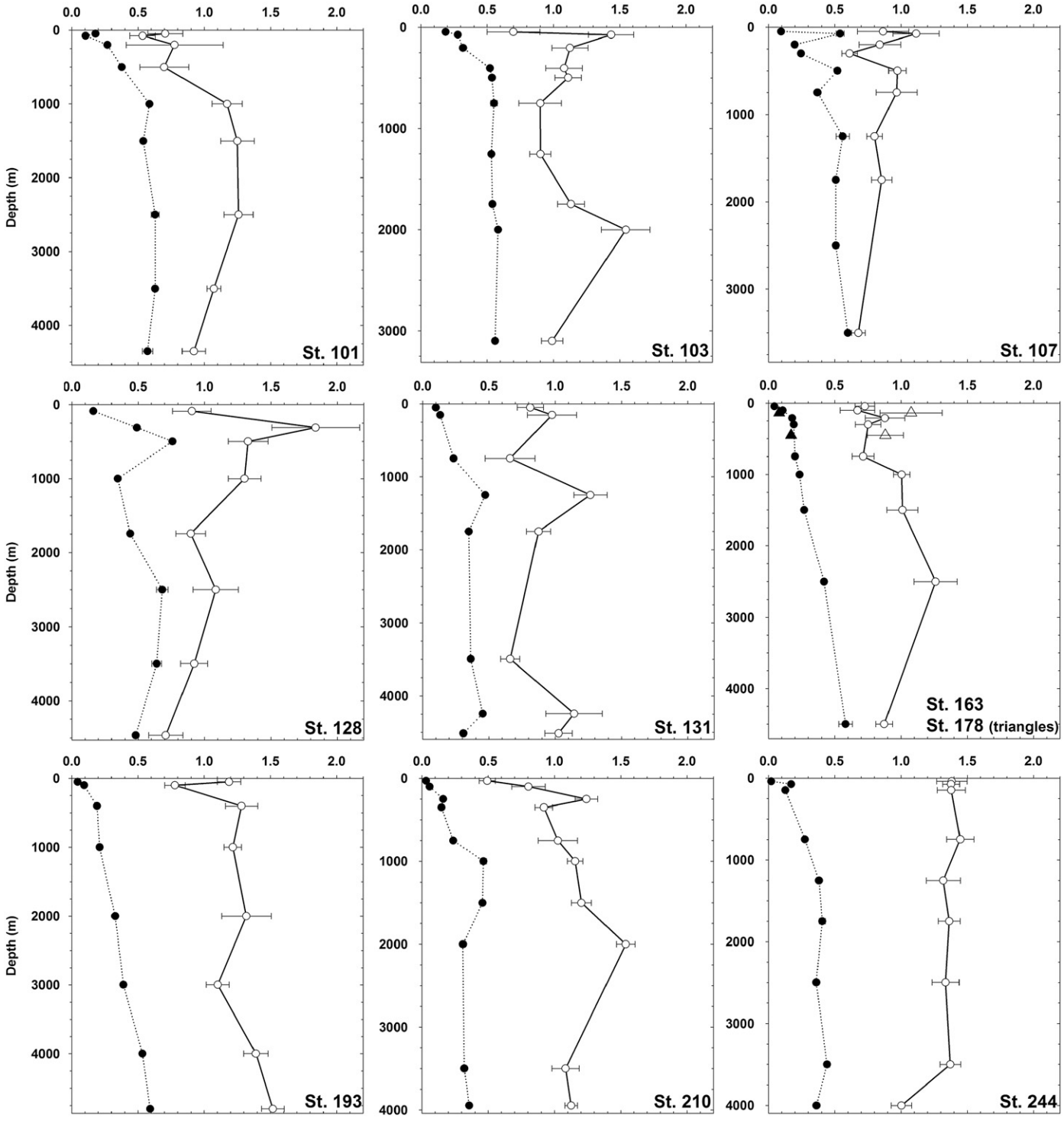

Fig. 2. Vertical distribution of organic ligands (white dots and solid line) and of dissolved Fe (black dots and dotted line) for the 10 stations. Station 163 and 178 (triangles at 137 and 451 m) are plotted in the same graph. Ligand concentrations are in nEq of M Fe and dissolved Fe concentrations are in nM. The vertical axes are extended until the bottom depth.

a decrease in pFe from 23.7–23.8 at the surface to 22.2–22.5 near the seafloor was found.

The ratio [Lt]/[dFe] (Figs. 3 and 4, Tables 2 and 3) shows how much more ligand there is compared to the dissolved Fe. If [Lt]/[dFe]=1, the ligand sites are fully saturated with Fe. The ratio [Lt]/[dFe] is a useful concept to highlight differences in ligand saturation throughout the water column and between different geographical locations (Thuróczy et al., 2010). In order to discuss separately the phenomena and processes occurring in the ocean, the boundary between the upper and deeper ocean was operationally defined at 450 m depth. This choice was dictated by the sampling depths, as the samples were usually taken at fixed depth (…400, 500, 750 m depth…).

A trend was seen in the [Lt]/[dFe] ratio with depth in the water column. High [Lt]/[dFe] ratio values were found at the surface with a decrease until 450 m (Figs. 3 and 4, Table 3). The upper layer (0–450 m) was characterised by low dissolved Fe concentrations (surface minima) and variable ligand concentrations.

Table 2
Dissolved Fe and the characteristics of the dissolved Fe-binding ligands of all samples. Dissolved Fe concentrations [dFe] are in nM (± standard deviations).

Station	Depth (m)	dFe (nM)	Std. dev.	[Lt] (nEq of M Fe)	Std. dev.	log K' (mol^{-1})	Std. dev.	[L'] (nEq of M Fe])	log α	pFe (M)	[Lt]/[dFe]
101											
	48	0.180	0.010	0.71	0.13	22.00	0.35	0.53	12.72	22.47	3.9
	76	0.105	0.007	0.53	0.10	22.12	0.24	0.43	12.76	22.73	5.1
	199	0.270	0.000	0.78	0.37	21.45	0.27	0.51	12.15	21.72	2.9
	502	0.377	0.004	0.70	0.18	21.69	0.33	0.32	12.19	21.62	1.9
	1001	0.587	0.017	1.17	0.11	21.66	0.09	0.59	12.43	21.66	2.0
	1502	0.540	0.020	1.25	0.13	22.16	0.21	0.71	13.02	22.28	2.3
	2501	0.630	0.030	1.26	0.11	21.91	0.13	0.63	12.71	21.91	2.0
	3505	0.630	0.000	1.07	0.05	22.61	0.20	0.44	13.26	22.46	1.7
	4353	0.572	0.039	0.92	0.09	22.42	0.29	0.35	12.97	22.21	1.6
103											
	45	0.187	0.005	0.70	0.20	22.39	0.41	0.51	13.10	22.82	3.7
	73	0.280	0.020	1.44	0.17	22.11	0.19	1.16	13.17	22.72	5.1
	203	0.318	0.015	1.12	0.14	22.40	0.25	0.81	13.30	22.80	3.5
	404	0.522	0.004	1.08	0.14	22.21	0.32	0.56	12.96	22.24	2.1
	499	0.536[a]	[b]	1.11	0.10	22.59	0.30	0.57	13.35	22.62	2.1
	751	0.551	0.025	0.90	0.16	22.18	0.35	0.35	12.72	21.98	1.6
	1253	0.532	0.008	0.90	0.08	22.38	0.26	0.37	12.94	22.22	1.7
	1747	0.540	[b]	1.13	0.10	22.74	0.28	0.59	13.51	22.78	2.1
	2001	0.582	0.009	1.55	0.18	21.93	0.18	0.96	12.92	22.15	2.7
	3099	0.560	0.006	0.99	0.08	22.34	0.22	0.43	12.98	22.23	1.8
107											
	49	0.096	0.002	0.87	0.19	21.84	0.36	0.77	12.73	22.75	9.1
	75	0.540	0.030	1.11	0.17	22.16	0.35	0.57	12.92	22.18	2.1
	199	0.199	0.008	0.84	0.16	21.69	0.16	0.64	12.50	22.20	4.2
	301	0.246	0.013	0.61	0.06	22.49	0.33	0.37	13.06	22.67	2.5
	499	0.520	0.020	0.97	0.07	22.31	0.17	0.45	12.96	22.25	1.9
	749	0.370	0.020	0.97	0.15	21.91	0.24	0.60	12.68	22.11	2.6
	1250	0.560	0.050	0.80	0.06	22.48	0.16	0.24	12.86	22.11	1.4
	1749	0.507	0.006	0.85	0.08	22.54	0.36	0.35	13.08	22.38	1.7
	3500	0.508	0.020	0.68	0.05	22.94	0.31	0.08	12.85	22.07	1.1
128											
	87	0.162	0.017	0.90	0.15	21.86	0.23	0.74	12.73	22.52	5.6
	311	0.490	0.010	1.84	0.33	21.74	0.23	1.35	12.87	22.18	3.8
	498	0.759	0.020	1.33	0.15	21.97	0.17	0.57	12.72	21.84	1.7
	1001	0.345	0.005	1.30	0.12	21.95	0.15	0.96	12.93	22.40	3.8
	1744	0.439	0.012	0.90	0.11	22.18	0.28	0.46	12.84	22.20	2.0
	2498	0.682	0.044	1.08	0.17	22.23	0.47	0.40	12.83	22.00	1.6
	3497	0.640	0.036	0.92	0.10	22.58	0.28	0.28	13.03	22.22	1.4
	4466	0.481	0.014	0.71	0.13	22.29	0.28	0.23	12.64	21.96	1.5
131											
	50	0.100	0.010	0.81	0.10	22.40	0.43	0.71	13.25	23.25	8.1
	152	0.133	0.003	0.98	0.19	21.68	0.21	0.84	12.60	22.48	7.3
	748	0.235	0.001	0.66	0.19	21.84	0.40	0.43	12.47	22.10	2.8
	1250	0.473	0.009	1.27	0.12	21.86	0.13	0.79	12.76	22.08	2.7
	1750	0.348	0.001	0.87	0.09	22.53	0.40	0.53	13.26	22.71	2.5
	3495	0.362	0.002	0.66	0.07	22.10	0.21	0.30	12.58	22.02	1.8
	4245	0.453	0.002	1.14	0.21	21.87	0.22	0.69	12.71	22.05	2.5
	4514	0.307	0.004	1.03	0.10	22.22	0.23	0.72	13.07	22.59	3.3
163											
	44	0.045	0.001	0.73	0.07	22.50	0.39	0.68	13.33	23.68	16.2
	101	0.107	0.006	0.67	0.13	22.16	0.54	0.56	12.91	22.88	6.3
	210	0.180	0.001	0.88	0.15	22.04	0.30	0.70	12.89	22.63	4.9
	300	0.192	0.001	0.75	0.10	22.32	0.35	0.56	13.07	22.78	3.9
	748	0.201	0.003	0.71	0.08	22.36	0.33	0.51	13.07	22.77	3.6
	1001	0.235	0.013	1.00	0.06	22.37	0.15	0.77	13.26	22.89	4.3
	1501	0.270	0.014	1.01	0.12	22.53	0.61	0.74	13.40	22.96	3.7
	2501	0.418	0.012	1.26	0.16	22.30	0.40	0.84	13.23	22.61	3.0
	4499	0.581	0.051	0.87	0.06	22.51	0.25	0.29	12.98	22.21	1.5
178											
	137	0.081	0.007	1.08	0.23	21.60	0.18	1.00	12.59	22.69	13.3
	451	0.171	0.005	0.88	0.14	21.93	0.24	0.71	12.79	22.55	5.2
193											
	50	0.045	0.001	1.33	0.17	22.20	0.35	1.28	13.31	23.66	26.7
	101	0.094	0.003	0.69	0.07	22.60	0.46	0.59	13.38	23.40	8.3
	402	0.192	0.009	1.31	0.13	22.24	0.25	1.11	13.29	23.00	6.7
	1000	0.211	0.006	1.25	0.11	22.18	0.19	1.04	13.20	22.87	5.8
	2001	0.327	0.002	1.32	0.19	22.12	0.26	0.99	13.12	22.60	4.0
	2998	0.390	0.021	1.10	0.09	22.76	0.55	0.71	13.61	23.02	2.8
	3997	0.534	0.003	1.39	0.09	22.43	0.21	0.86	13.36	22.63	2.6
	4799	0.592	0.015	1.52	0.09	22.34	0.16	0.93	13.31	22.53	2.6

Table 2 (*continued*)

Station	Depth (m)	dFe (nM)	Std. dev.	[Lt] (nEq of M Fe)	Std. dev.	log K' (mol^{-1})	Std. dev.	[L'] (nEq of M Fe])	log α	pFe (M)	[Lt]/[dFe]
210											
	30	0.030	0.010	0.49	0.06	22.56	0.43	0.46	13.22	23.73	15.8
	99	0.060	0.010	0.80	0.13	22.16	0.46	0.75	13.04	23.28	13.9
	249	0.160	0.000	1.24	0.09	22.34	0.20	1.08	13.37	23.16	7.7
	351	0.150	0.010	0.92	0.06	22.23	0.16	0.77	13.12	22.94	6.2
	750	0.240	0.010	1.03	0.15	22.17	0.21	0.79	13.07	22.70	4.3
	1000	0.460	0.020	1.16	0.06	22.64	0.23	0.69	13.48	22.81	2.5
	1501	0.460	0.020	1.20	0.07	22.44	0.12	0.75	13.31	22.66	2.6
	2000	0.310	0.020	1.54	0.07	22.24	0.10	1.23	13.33	22.84	5.0
	3500	0.320	0.010	1.08	0.10	22.12	0.19	0.76	13.00	22.50	3.4
	3946	0.360	0.010	1.13	0.05	22.34	0.11	0.77	13.22	22.67	3.2
244											
	38	0.021	0.001	1.38	0.11	21.90	0.12	1.36	13.03	23.71	66.9
	73	0.172	0.005	1.38	0.06	22.78	0.30	1.21	13.87	23.63	8.0
	147	0.128	0.011	1.38	0.11	22.30	0.22	1.25	13.40	23.29	10.8
	748	0.276	0.005	1.45	0.10	22.14	0.15	1.17	13.21	22.76	5.2
	1250	0.381	0.007	1.32	0.13	22.50	0.36	0.94	13.47	22.89	3.5
	1749	0.405	0.024	1.36	0.08	22.11	0.12	0.96	13.09	22.48	3.4
	2497	0.361	0.019	1.34	0.10	22.16	0.16	0.98	13.15	22.59	3.7
	3501	0.441	0.021	1.37	0.08	22.18	0.12	0.93	13.15	22.51	3.1
	4002	0.362	0.002	1.00	0.08	22.59	0.33	0.64	13.40	22.84	2.8

Concentrations of the ligand [Lt] and the excess ligand [L'] are in nEq of M Fe ($\pm$ standard deviations).
Conditional stability constants K' are in mol^{-1} with standard deviations.
$[L'] = ([Lt] - [dFe])$.
$\alpha_{organic} = [L'] K'$.
$pFe = -\log \{[dFe]/(\alpha_{inorganic} + \alpha_{organic})\}$ (M).
At station 101 the deepest samples collected at 3505 and 4353 m had higher values of dissolved Fe, 0.630 and 0.572 nM, respectively, as compared with the duplicate subsamples reported by Klunder et al. (2011), 0.401 and 0.280 nM, respectively. The cause for this discrepancy is not known; perhaps our samples were contaminated. Nevertheless here we use our values, 0.63 and 0.572 nM in further interpretation. At station 178 Klunder et al. (2011) measured a complete vertical profile and found elevated concentrations of dissolved Fe between 300 and 800 m depth due to melted ice (1.50 nM of Fe at 451 m). The cause for the discrepancy with our sample at 451 m (0.171 nM) is not known.

[a] When the [dFe] was not determined in the same sample and therefore the concentration [dFe] was averaged from the samples above and under it; this was used for the calculation of the ligand characteristics (Eq. (2)).

[b] The standard deviation for Fe concentrations is missing when there were not enough samples to determine the concentration in triplicate.

To highlight the steep decrease of the ratio [Lt]/[dFe] from the upper layer downwards, the ratios of the samples from the surface, i.e. the samples where phytoplankton grew (fluorescence > 0.1 a.u., Table 1) and of the layer underneath until 450 m depth (fluorescence < 0.1 a.u.) are shown separately in Table 3C. Below 450 m depth the ratios [Lt]/[dFe] were lower and more constant with depth. This deeper part appeared to be a relatively stable environment (constant concentrations of dissolved Fe and of ligand) where degradation and remineralisation of the organic matter were the dominant chemical processes. A trend in [Lt]/[dFe] between geographical locations was also seen (Figs. 3 and 4, Table 3). The ratio values [Lt]/[dFe] increased in average over the whole water column southwards the Southern Boundary on the Zero Meridian and from east to west in the Weddell Gyre.

4. Discussion

4.1. Comparison with literature

The ligand concentrations presented here are similar to the 0.4 and 1.4 nEq of M Fe reported for the upper 1000 m at 2 stations close to the ice edge at 0° and 10°W by Boye et al. (2001) and along the 20°E in the ACC. Surface water (until 100 m depth) ligand and Fe concentrations published by Boye et al. (2005) from the EisenEx experiment were also comparable at 0.5–0.7 nEq of M Fe and 0.05 nM, respectively. In addition, similar Fe speciation was estimated (between 0.5 and 1.5 nEq of M Fe) for the Kerguelen Archipelago Plateau in the Southern Ocean by Gerringa et al. (2008), with the exception of the deepest samples. These higher ligand concentrations at depth were attributed to the influence of the sediments. Only at station 131 were the ligand concentrations found below 4000 m similar to those measured by Gerringa et al. (2008).

The K' values for the entire water column calculated by Gerringa et al. (2008) using the same method were lower ($< 10^{22}$) than the K' values estimated here (mainly $> 10^{22}$). At 55°49′S–6°1′E Croot et al. (2004a, 2004b) found, below a surface minimum (1 nEq of M Fe), a decrease in the concentration of ligand from 2.5 nEq of M Fe at 30 m depth to 1.2 nEq of M Fe at 400 m. This result is comparable to station 128 located in the same area. The K' values found by Croot et al. (2004a, 2004b) were also similar (around 10^{22}) to those found here in the upper 400 m. The dissolved organic ligand characteristics observed during the present study and by others (Powell and Donat, 2001; Gerringa et al., 2008) did not indicate differences between water masses.

4.2. Upper layer of the ocean (0–450 m)

The trend of an increasing [Lt]/[dFe] ratio in the upper waters (Tables 3A and C, Fig. 4) from north to south on the Zero Meridian and from east to west in the Weddell Gyre probably reflects the existing phytoplankton regimes (Sub-Antarctic region and HNLC region). The high surface ratio confirms the importance of phytoplankton in increasing the ratio [Lt]/[dFe], by Fe uptake and probably ligand production. Both the concentrations of dissolved Fe and of ligands explain the difference in ratios [Lt]/[dFe], lower north of the SB and higher in the Weddell Gyre. Within the Weddell Gyre, the increase in [Lt]/[dFe] ratio from east to west was due to a decrease in

Table 3
Average and standard deviation of [Lt] (nEq of M Fe), [dFe] (nM), [L'] (nEq of M Fe) and the ratio [Lt]/[dFe] per station and per zone; (A) in the upper layer (0–450 m), (B) in the deeper part of the ocean (below 450 m depth) and (C) subdivision of the upper layer for [Lt]/[dFe]: samples from the surface are shown separately from those in the euphotic layer (where fluorescence >0.1 a.u., surface sample included) and in the layer below it until 450 m depth (intermediate layer).

A			Upper layer (0–450 m)								
Zones		**Stations**	**Number of samples**	**Average [Lt]**	**Std. dev.**	**Average [dFe]**	**Std. dev.**	**Average [L']**	**Std. dev.**	**Average [Lt]/[dFe]**	**Std. dev.**
↑	**North of SB**	**101**	$n=3$	0.67	0.12	0.185	0.083	0.49	0.05	4.0	1.1
		103	$n=4$	1.08	0.30	0.327	0.141	0.76	0.29	3.6	1.2
		107	$n=4$	0.86	0.21	0.270	0.191	0.59	0.17	4.5	3.2
		Average	$n=11$	**0.89**	**0.27**	**0.267**	**0.147**	**0.62**	**0.22**	**4.0**	**2.0**
Prime Meridian	↑	**128**	$n=2$	1.37	0.66	0.326	0.232	1.04	0.43	4.7	1.3
		131	$n=2$	0.89	0.12	0.116	0.023	0.78	0.09	7.7	0.6
		163	$n=4$	0.76	0.09	0.131	0.068	0.63	0.07	7.8	5.7
		178	$n=2$	0.98	0.14	0.126	0.064	0.85	0.20	9.2	5.8
↓	**Weddell Gyre**	**Average**	$n=10$	**0.95**	**0.33**	**0.166**	**0.123**	**0.79**	**0.23**	**7.5**	**4.1**
Weddell Sea		**193**	$n=3$	1.08	0.27	0.110	0.075	0.97	0.25	13.9	11.1
		210	$n=4$	0.86	0.31	0.099	0.064	0.77	0.25	10.9	4.7
	↓	**Average**	$n=7$	**0.96**	**0.29**	**0.104**	**0.063**	**0.85**	**0.26**	**12.2**	**7.4**
Drake Passage		**244**	$n=3$	1.29	0.18	0.131	0.079	1.27	0.08	28.6	33.2[a]

B			Deeper layer (below 450 m)								
Zones		**Stations**	**Number of samples**	**Average [Lt]**	**Std. dev.**	**Average [dFe]**	**Std. dev.**	**Average [L']**	**Std. dev.**	**Average [Lt]/[dFe]**	**Std. dev.**
↑	**North of SB**	**101**	$n=6$	1.06	0.22	0.556	0.094	0.51	0.16	1.9	0.3
		103	$n=6$	1.10	0.24	0.550	0.019	0.55	0.23	2.0	0.4
		107	$n=5$	0.85	0.12	0.511	0.077	0.34	0.20	1.7	0.6
		Average	$n=17$	**1.01**	**0.22**	**0.539**	**0.070**	**0.47**	**0.20**	**1.9**	**0.4**
Prime Meridian	↑	**128**	$n=6$	1.04	0.24	0.558	0.160	0.48	0.26	2.0	0.9
		131	$n=6$	0.94	0.25	0.363	0.089	0.58	0.19	2.6	0.5
		163	$n=5$	0.97	0.20	0.341	0.158	0.63	0.23	3.2	1.1
↓	**Weddell Gyre**	**Average**	$n=17$	**0.98**	**0.22**	**0.425**	**0.164**	**0.56**	**0.22**	**2.6**	**0.9**
Weddell Sea		**193**	$n=5$	1.25	0.20	0.376	0.162	0.90	0.12	3.6	1.4
		210	$n=6$	1.19	0.18	0.357	0.089	0.83	0.20	3.5	1.0
	↓	**Average**	$n=11$	**1.24**	**0.17**	**0.382**	**0.119**	**0.86**	**0.16**	**3.5**	**1.1**
Drake Passage		**244**	$n=6$	1.31	0.16	0.371	0.055	0.94	0.17	3.6	0.9

C			Subdivision of the upper 450 m in								
			Surface sample			**Euphotic layer (where fluorescence >0.1 a.u.)**			**Intermediate layer (where fluorescence <0.1 a.u.)**		
Zones		**Stations**	**Depth (m)**	**Number of samples**	**[Lt]/[dFe]**	**Depth (m)**	**Number of samples**	**Average [Lt]/[dFe]**	**Depth (m)**	**Number of samples**	**Average [Lt]/[dFe]**
↑	**North of SB**	**101**	48	$n=1$	3.9	0–100	$n=2$	4.5 ± 0.8	100–450	$n=1$	2.9
		103	45	$n=1$	3.7	0–75	$n=2$	4.4 ± 1.0	75–450	$n=2$	2.8 ± 1.0
		107	49	$n=1$	9.1	0–100	$n=2$	5.6 ± 4.9	100–450	$n=2$	3.4 ± 1.2
		Average		$n=3$	**5.6 ± 3.0**		$n=6$	**4.8 ± 2.4**		$n=5$	**3.0 ± 0.9**
Prime Meridian	↑	**128**	87	$n=1$	5.6	0–90	$n=1$	5.6	90–450	$n=1$	3.8
		131	50	$n=1$	8.1	0–100	$n=1$	8.1	100–450	$n=1$	7.3
		163	44	$n=1$	16.2	0–100	$n=2$	11.2 ± 7.0	100–450	$n=2$	4.4 ± 0.7
		178				0–140	$n=1$	13.3	140–450	$n=1$	5.2
↓	**Weddell Gyre**	**Average**		$n=3$	**10.0 ± 5.5**		$n=5$	**9.9 ± 4.6**		$n=5$	**5.0 ± 1.4**
Weddell Sea		**193**	50	$n=1$	26.7	0–100	$n=2$	17.5 ± 13	100–450	$n=1$	6.7
		210	30	$n=1$	15.8	0–50	$n=1$	15.8	50–450	$n=3$	9.3 ± 4.2
	↓	**Average**		$n=2$	**21.2 ± 7.7**		$n=3$	**16.9 ± 9.2**		$n=4$	**8.6 ± 3.6**
Drake Passage		**244**	38	$n=1$	66.9	0–100	$n=2$	37.5 ± 41.6[a]	100–450	$n=1$	10.8

[a] Indicates large standard deviation (Station 244) due to the extremely high surface ratio [Lt]/[dFe] (66.9) compared to the value below this.

the concentration of dissolved Fe only. Lower concentrations of dissolved Fe were found in the Weddell Sea proper (0.10 nM, $n=7$) as compared to those found in the Weddell Gyre on the Zero Meridian (0.17 nM, $n=10$). The concentrations of ligand and excess L were relatively constant in the Weddell Gyre. The values of organic alpha and pFe also showed a trend in the upper layer between

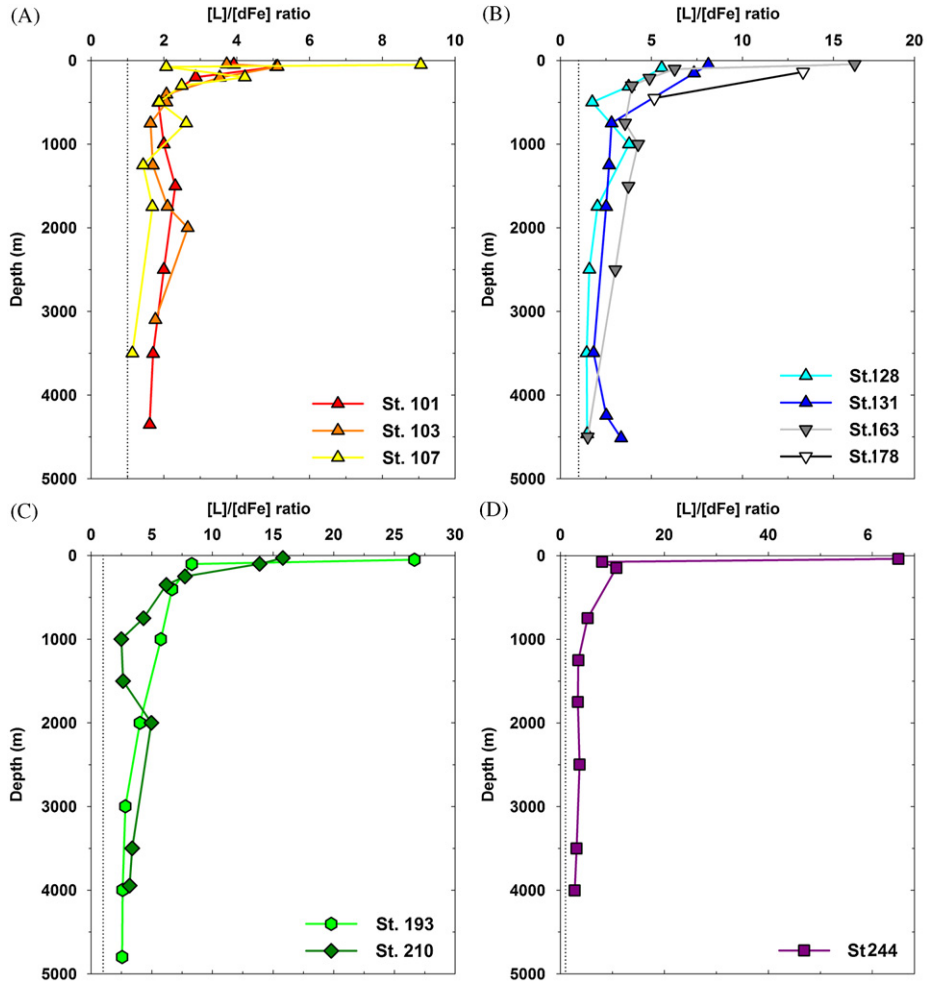

Fig. 3. Ratio values of [Lt]/[dFe]. (A) North of the SB; (B) Weddell Gyre on the Zero Meridian; (C) Weddell Sea and (D) Drake Passage. The dotted line marks exact saturation of the ligand with [Lt]/[dFe]=1. Note the different scales on the horizontal axis for the ratio values.

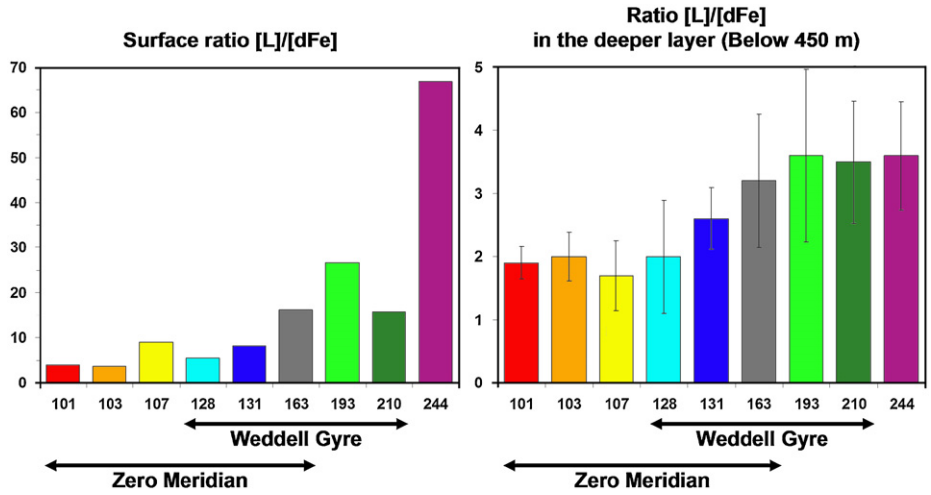

Fig. 4. Values of [Lt]/[dFe] per station. On the left side: surface values of [Lt]/[dFe]. On the right side: averaged values of [Lt]/[dFe] with standard deviations in the layer below 450 m depth. Station 178 is not shown here since only 2 samples were taken (137 and 451 m depth).

geographical locations. The increase of organic alpha from north to south on the Zero Meridian and from east to west in the Weddell Gyre was due to an increase in excess *L*, whereas the increase in pFe value in the upper layer was due to a decrease of the dissolved Fe concentration and an increase of the organic alpha. Station 244, located in the Drake Passage, showed the highest [Lt]/[dFe] ratio at the surface caused by both a high ligand concentration relative to a very low dissolved Fe concentration (0.021 nM). The trend of the

ratio [Lt]/[dFe] between geographical locations is seen in the ratio [Lt]/[dFe] of the surface samples (0–50 m) (Table 3C), but also in the euphotic layer (fluorescence >0.1 a.u.) and in the layer below this (fluorescence <0.1 a.u.).

The high [Lt]/[dFe] at the surface can be explained by the uptake of Fe and production of ligands (relatively high and variable ligand concentrations) by phytoplankton in the euphotic layer and by the microbial activity degrading the non-resistant ligands (Rue and Bruland, 1997; Tortell et al., 1999; Boye and van den Berg, 2000; Croot et al., 2001; Gerringa et al., 2006). The ligand concentration represents the difference between the production and the degradation of the Fe-binding molecules (Boye et al., 2001).

The stations were located in regions influenced by different "regimes" in terms of primary production. The regime in the surface waters at stations 101, 103 and 107 (Sub-Antarctic region) is thus very different from the other stations. Relatively low [Lt]/[dFe] ratio values were found at these stations. Relatively high fluorescence was measured here and Fe was not a limiting factor for phytoplankton growth at these 3 stations. Moreover, the dissolved organic ligand concentration was lower here. This indicated that there was no (need for) production of ligands like siderophores by the prokaryotes.

The stations located in the HNLC regions (128, 131, 163, 178, 193 and 210) had low dissolved Fe concentrations and relatively constant ligand concentrations, resulting in higher [Lt]/[dFe] ratio values. Near the edge of the Antarctic ice sheet even higher [Lt]/[dFe] ratio values were found. Here a phytoplankton bloom was clearly observed by high fluorescence at station 163 and 178 (Table 1): a source of Fe was apparently available since the bloom had started. The melting of the Antarctic ice sheet, its calving icebergs and of the seasonal sea-ice was shown to be a source of dissolved Fe in seawater by Klunder et al. (2011). This extra Fe was consumed resulting in low dissolved Fe concentrations. Here, the ligand concentration was relatively constant and was not responsible for the high [Lt]/[dFe] ratio values. However, in the Weddell Sea, even higher ratios [Lt]/[dFe] were found at the surface, whereas, the fluorescence in the water was low. Low dissolved Fe concentrations occurring here explained this high ratio [Lt]/[dFe]. The low dissolved Fe concentration might be caused by a phytoplankton bloom in the recent past or more probably Fe is taken up by phytoplankton living in the sea-ice. The Weddell Sea is known to be a productive area with high biological diversity supported by the growth of phytoplankton in the sea-ice (Arrigo et al., 1997; Flores, 2009). So, even if relatively low fluorescence was measured in the water, Fe consumption should be high.

The particulate fraction, an important part of the Fe cycle, is still missing in the present study and should help to explain the processes occurring in the upper ocean. Adsorption sites on suspended particles compete with empty ligand sites in the dissolved fraction for Fe (Thuróczy et al., 2010). The adsorption on suspended particles followed by aggregation and downward settling of these particles is deemed to be responsible for the removal of Fe by scavenging.

4.3. Deeper part of the ocean (below 450 m)

Below 450 m depth, the values of [Lt]/[dFe] were low and constant with depth. Like the upper layer (0–450 m depth), the deeper part of the water column also showed a geographical trend: an increase of the ratio [Lt]/[dFe] southwards the Southern Boundary on the Zero Meridian and from east to west in the Weddell Gyre.

The difference between Zero Meridian and Weddell Sea was due to a lower concentration of ligand (1.00 of nEq of M Fe, $n=34$; versus 1.24 nEq of M Fe, $n=11$, respectively). The southward decrease in dissolved Fe concentration on the Zero Meridian was due to an absence of Fe sources (Klunder et al., 2011). Moreover, excess L increased southwards along the Zero Meridian, thus reinforcing the same trend in [Lt]/[dFe]. Within the Weddell Gyre, the increase of [Lt]/[dFe] ratios from east to west was caused by both the concentrations of dissolved Fe (decrease) and the ligand concentration (increase). Obviously the excess ligand concentration also increased from east to west in the Weddell Gyre resulting in the increase of organic alpha value and combined with the decrease in the dissolved Fe concentration, an increase in pFe. Finally, the relatively high ratios of [Lt]/[dFe] in the deep part of the Drake Passage were due to high concentrations of ligand (1.31 nEq of M Fe, $n=6$) and remarkably constant excess L with depth.

The ratio [Lt]/[dFe] was constant below 450 m. Hunter and Boyd (2007) suggested that Fe-binding ligands in the deep ocean are refractory humic materials that originate from degradation of organic matter in the surface layer. The degradation would generate ligand functional groups in the deep ocean (Kuma et al., 1996; Chen et al., 2003) where only one dominant group of ligands is present (Rue and Bruland, 1995; Hunter and Boyd, 2007). The ligand characteristics found in the deep ocean in our samples were indeed relatively constant with depth (constant pFe and organic alpha reflecting an equilibrium between ligands, precipitation and adsorption of Fe) or showed a slight vertical trend, with increasing depth a decrease of excess L, and slight increase of K' value (Tables 2 and 3; Figs. 2–4). The ligand characteristics in the deep ocean reflect either a balance between production and degradation of dissolved organic ligands or a constant very refractory type/group of ligands. If constant production of ligands by microbial activity with depth exists (Reid et al., 1993) it must be balanced by a constant degradation of ligands (Powell and Donat, 2001). Witter and Luther (1998) showed with a kinetic approach a change in the formation rate of Fe–ligand complexes and consequently the change of the dissociation rate (slower in the deep). They suggested that very slow degradation of ligands results in long residence time of the ligands (up to 1000 yr). Our data could confirm this statement since the southward flowing water is depleted in Fe but not in ligand: Our study showed a uniform concentration of dissolved organic ligand and a rather uniform K' in deep waters, causing constant organic alpha and pFe values, not suggesting transformation of ligand characteristics with time as suggested by Witter and Luther (1998). Since the trend in [Lt]/[dFe] ratio in the deep waters between geographical locations (Figs. 1, 3 and 4, Table 3) was a consequence of what happened in the surface layer, the export of particulate organic matter is important. Knowledge of Fe in other size fractions, like the particulate fraction from unfiltered water and different colloidal size fractions would help to understand which processes control the ligands and the Fe distribution in the deep ocean.

5. Conclusions

Overall the observed trends in [Lt]/[dFe] ratio values with depth and geographical location were consistent with the changes in ligand characteristics (excess L, organic alpha and resulting pFe) but showed a much clearer trend than the separate other parameters and confirmed that the ratio [Lt]/[dFe] is a reliable concept to study the chemistry of Fe in the oceans. This study has shown clear differences between upper waters (until 450 m depth), influenced by the presence of the phytoplankton, and deeper waters (below 450 m depth) in dissolved organic ligand characteristics and in the distribution of dissolved Fe. These high ratios (3.7–66.9) at the surface decreased to a nearly constant

value below 450 m (1.7–3.6). Both the upper (0–450 m) and deeper (below 450 m) parts of the ocean showed an increasing trend southwards. In the upper 450 m this trend reflected the increasing depletion of Fe resulting in HNLC waters with increasing distance from Fe sources. However, the ligands also showed an increasing trend southwards showing that they are very resistant to degradation. In the upper layer of the Weddell Gyre, the increase in [Lt]/[dFe] ratio values from east to west is due to a decrease in dissolved Fe concentrations. In the deeper waters of the Weddell Gyre it is due to both the increase of ligand and the decrease of dissolved Fe concentrations. In the deep waters (below 450 m depth) a steady state between dissolved organic ligand and dissolved Fe was found at any location reflecting a balance between production and degradation of the organic matter. With the increase of dissolved Fe concentrations with depth, the ligand sites for binding Fe are getting filled, and even almost saturated (North of the SB on the Zero Meridian). This near saturation is deemed to be consistent with the precipitation of Fe as insoluble oxyhydroxide and its removal to the deep ocean. It confirms the important role of the organic ligands in keeping Fe in the soluble phase, thus avoiding its precipitation, and increasing its residence time in the water column. In the deeper layer (>450 m) the increase in the [Lt]/[dFe] ratio is caused by a decrease in dissolved Fe concentrations only. A consistent trend in [Lt]/[dFe] values, at various depths and locations, is in itself impressive since nobody, to our knowledge, ever found clear trends in ligand characteristics other than a general decrease in ligand concentration with depth. However, the explanation is not still completely clear. The competition in the overall Fe budget between stabilisation by organic ligands and the removal by scavenging (adsorption onto particulate matter and colloid aggregation with or without oxidative precipitation) needs to be taken into account in order to better understand the Fe cycle in the ocean.

Acknowledgments

The authors are very grateful to Captain S. Schwarze of *Polarstern* and his crew for their help and would like to thank Jan van Ooijen and Sven Ober from the Royal-NIOZ for the data of the nutrients and the CTD, respectively. Three anonymous reviewers are gratefully thanked for their helpful comments. We also thank Claire Evans for her help with improving the English editing.

In memory of Willem Polman, we will never forget his great helping hand. Special thanks to Michael Stimac for his voluntary help in our team.

This work was funded by the International Polar Year programme of the Netherlands Organisation for Scientific Research (NWO) as the subsidy for Geotraces sub-project 851.40.102 entitled Physical and chemical speciation of dissolved iron in Polar Oceans.

References

Alldredge, A., Passow, U., Logan, B., 1993. The abundance and significance of a class of large, transparent organic particles in the ocean. Deep-Sea Research I 40 (6), 1131–1140.

Arrigo, K.R., Worthen, D.L., Lizotte, M.P., Dixon, P., Dieckmann, G., 1997. Primary Production in Antarctic Sea Ice. Science 276 (5311), 394–397. doi:10.1126/science.276.5311.394.

de Baar, H.J.W., Buma, A.G.J., Nolting, R.F., Cadée, G.C., Jacques, G., Tréguer, P.J., 1990. On iron limitation of the Southern Ocean: experimental observations in the Weddell and Scotia Seas. Marine Ecology Progress Series 65 (2), 105–122.

de Baar, H.J.W., de Jong, J.T.M., Bakker, D.C.E., Löscher, B.M., Veth, C., Bathmann, U., Smetacek, V., 1995. Importance of iron for plankton blooms and carbon dioxide drawdown in the Southern Ocean. Nature 373 (6513), 412–415.

de Baar, H.J.W., Timmermans, K.R., Laan, P., de Porto, H.H., Ober, S., Blom, J.J., Bakker, M.C., Schilling, J., Sarthou, G., Smit, M.G., Klunder, M., 2008. Titan: A new facility for ultraclean sampling of trace elements and isotopes in the deep oceans in the international Geotraces program. Marine Chemistry 111 (1–2), 4–21.

Babin, M., Morel, A., Gentili, B., 1996. Remote sensing of sea surface Sun-induced chlorophyll fluorescence: Consequences of natural variations in the optical characteristics of phytoplankton and the quantum yield of chlorophyll *a* fluorescence. International Journal of Remote Sensing 17 (12), 2417–2448.

Barré, N., Provost, C., Sennechael, 2008. Circulation in the Ona Basin, southern Drake Passage. Journal of Geophysical Research 113 (C4), C04033. doi:10.1029/2007JC004549.

Boye, M., van den Berg, C.M.G., 2000. Iron availability and the release of iron-complexing ligands by *Emiliania huxleyi*. Marine Chemistry 70 (4), 277–287.

Boye, M., van den Berg, C.M.G., de Jong, J.T.M., Leach, H., Croot, P., de Baar, H.J.W., 2001. Organic complexation of iron in the Southern Ocean. Deep-Sea Research I 48 (6), 1477–1497.

Boye, M., Nishioka, J., Croot, P.L., Laan, P., Timmermans, K.R., de Baar, H.J.W., 2005. Major deviations of iron complexation during 22 days of a mesoscale iron enrichment in the open Southern Ocean. Marine chemistry 96 (3–4), 257–271.

Buma, A.G.J., de Baar, H.J.W., Nolting, R.F., Vanbennekom, A.J., 1991. Metal enrichment experiments in the Weddell-Scotia Seas—effects of iron and manganese on various plankton communities. Limnology and Oceanography 36 (8), 1865–1878.

Chen, M., Wang, W.-X., Guo, L., 2003. Phase partitioning and solubility of iron in natural seawater controlled by dissolved organic matter. Global Biogeochemistry Cycles 18 (4), GB 4013.

Coale, K.H., Johnson, K.S., Fitzwater, S.E., Gordon, R.M., Tanner, S., Chavez, F.P., Ferioli, L., Sakamoto, C., Rogers, P., Millero, F., Steinberg, P., Nightingale, P., Cooper, D., Cochlan, W.P., Landry, M.R., Constantinou, J., Rollwagen, G., Trasvina, A., Kudela, R., 1996. A massive phytoplankton bloom induced by an ecosystem-scale iron fertilization experiment in the equatorial Pacific Ocean. Nature 383 (6600), 495–501.

Croot, P.L., Johanson, M., 2000. Determination of iron speciation by cathodic stripping voltammetry in seawater using the competing ligand 2-(2-Thiazolylazo)-p-cresol (TAC). Electroanalysis 12 (8), 565–576.

Croot, P.L., Bowie, A.R., Frew, R.D., Maldonado, M.T., Hall, J.A., Safi, K.A., La Roche, J., Boyd, P.W., Law, C.S., 2001. Retention of dissolved iron and Fe-II in an iron induced Southern Ocean phytoplankton bloom. Geophysical Research Letters 28 (18), 3425–3428.

Croot, P.L., Streu, P., Baker, A.R., 2004a. Short residence time for iron in the surface seawater impacted by atmospheric dry deposition from Saharan dust events. Geophysical Research Letters 31 (23), L23S08.

Croot, P.L., Andersson, K., Öztürk, M., Turner, D.R., 2004b. The distribution and speciation of iron along 6°E in the Southern Ocean. Deep-Sea Research II 51 (22–24), 2857–2879.

Cullen, J.T., Bergquist, B.A., Moffett, J.W., 2006. Thermodynamic characterization of the partitioning of iron between soluble and colloidal species in the Atlantic Ocean. Marine Chemistry 98 (2–4), 295–303.

Fitzwater, S.E., Coale, K.H., Gordon, R.M., Johnson, K.S., Ondrusek, M.E., 1996. Iron deficiency and phytoplankton growth in the equatorial Pacific. Deep-Sea Research II 43 (4–6), 995–1015.

Flores, H., 2009. Frozen desert alive. Ph.D. Thesis, University of Groningen, The Netherlands. Electronic version available at: 〈http://www.rug.nl/bibliotheek/catalogibestanden/elekpubrug/dissertaties/index〉.

GEOTRACES Planning Group, 2006. GEOTRACES Science Plan. Scientific Committee on Oceanic Research, Baltimore, Maryland.

Gerringa, L.J.A., Herman, P.M.J., Poortvliet, T.C.W., 1995. Comparison of the linear van den Berg/Ružić transformation and a non-linear fit of the Langmuir isotherm applied to Cu speciation data in the estuarine environment. Marine Chemistry 48 (2), 131–142.

Gerringa, L.J.A., Veldhuis, M.J.W., Timmermans, K.R., Sarthou, G., de Baar, H.J.W., 2006. Co-variance of dissolved Fe-binding ligands with phytoplankton characteristics in the Canary Basin. Marine Chemistry 102 (3–4), 276–290.

Gerringa, L.J.A., Blain, S., Laan, P., Sarthou, G., Veldhuis, M.J.W., Brussaard, C.P.D., Viollier, E., Timmermans, K.R., 2008. Fe-binding organic ligands near the Kerguelen Archipelago in the Southern Ocean (Indian sector). Deep-Sea Research II 55, 606–621.

Gledhill, M., van den Berg, C.M.G., 1994. Determination of complexation of iron (III) with natural organic complexing ligands in sea water using cathodic stripping voltammetry. Marine Chemistry 47 (1), 41–54.

Grashoff, K., Erhardt, M., Kremling, K., 1983. Methods in Seawater Analyses. Verlag Chemie, Weinheim, Germany 419 pp.

Hudson, R.J.M., Rue, R.L., Bruland, K.W., 2003. Modeling complexometric titrations of natural water samples. Environmental Science and Technology 37, 1553–1562. doi:10.1021/ES025751A.

Hunter, K.A., Boyd, P.W., 2007. Iron-binding ligands and their role in the ocean biogeochemistry of iron. Environmental Chemistry 4 (4), 221–232. doi:10.1071/EN07012.

de Jong, J.T.M., den Das, J., Bathmann, U., Stoll, M.H.C., Kattner, G., Nolting, R.F., de Baar, H.J.W., 1998. Dissolved iron at subnanomolar levels in the Southern Ocean as determined by ship-board analysis. Analytica Chimica Acta 377 (2–3), 113–124.

Kepkay, P.E., 1994. Particle aggregation and the biological reactivity of colloids. Marine Ecology Progress Series 109 (2–3), 293–304.

Kiefer, D.A., 1973. Chlorophyll *a* fluorescence in marine centric diatoms: responses of chloroplasts to light and nutrient stress. Marine Biology 23 (1), 39–46.

Klunder, M.B., Laan, P., Middag, R., de Baar, H.J.W., van Ooijen, J.C, 2011. Dissolved Fe in the Southern Ocean (Atlantic sector). Deep-Sea Research II 58, 2678–2694.

Kuma, K., Nishioka, J., Matsunaga, K., 1996. Controls on iron(III) hydroxide solubility in seawater: the influence of pH and natural organic chelators. Limnology and Oceanography 41 (3), 396–407.

Logan, B.E., Passow, U., Alldredge, A.L., Grossart, H.-P., Simon, M., 1995. Rapid formation and sedimentation of large aggregates is predictable from aggregation rates (half lives) of transparent exopolymer particles (TEP). Deep-Sea Research II 42 (1), 203–214.

Lohan, M.C., Aguilar-Islas, A.M., Franks, R.P., Bruland, K.W., 2005. Determination of iron and copper in seawater at pH 1.7 with a new commercially available chelating resin, NTA superflow. Analytica Chimica Acta 530 (1), 121–129.

Martin, J.H., Gordon, R.M., 1988. Northeast Pacific iron distributions in relation to phytoplankton productivity. Deep-Sea Research 34 (2), 177–196.

Martin, J.H., Gordon, R.M., Fitzwater, S.E., 1991. The case for iron. Limnology and Oceanography 36 (8), 1793–1802.

Middag, R., de Baar, H.J.W., Laan, P., Baker, K., 2009. Dissolved aluminium and the silicon cycle in the Arctic Ocean. Marine Chemistry 115 (3–4), 176–195.

Middag, R., De Baar, H.J.W., Laan, P., Cai, P., Van Ooijen, J.C, 2011. Dissolved Manganese in the Atlantic sector of the Southern Ocean. Deep-Sea Research II 58, 2661–2677.

Millero, F.J., 1998. Solubility of Fe(III) in seawater. Earth and Planetary Science Letters 154 (1–4), 323–329.

Nolting, R.F., Gerringa, L.J.A., Swagerman, M.J.W., Timmermans, K.R., de Baar, H.J.W., 1998. Fe(III) speciation in the high nutrient, low chlorophyll Pacific region of the Southern Ocean. Marine Chemistry 62 (3–4), 335–352.

Pollard, R.T., Lucas, M.I., Read, J.F., 2002. Physical controls on biogeochemical zonation in the Southern Ocean. Deep-Sea Research II 49 (16), 3289–3305.

Powell, R.T., Donat, J.R., 2001. Organic complexation and speciation of iron in the South and Equatorial Atlantic. Deep-Sea Research II 48 (13), 2877–2893.

Reid, R.T., Live, D.H., Faulkner, D.J., Butler, A., 1993. A siderophore from a marine bacterium with an exceptional ferric ion affinity constant. Nature 366 (6454), 455–458.

Rue, E.L., Bruland, K.W., 1995. Complexation of iron(III) by natural organic ligands in the Central North Pacific as determined by a new competitive ligand equilibration/adsorptive cathodic stripping voltammetric method. Marine Chemistry 50 (1–4), 117–138.

Rue, E.L., Bruland, K.W., 1997. The role of organic complexation on ambient iron chemistry in the equatorial Pacific Ocean and the response of a mesoscale iron addition experiment. Limnology and Oceanography 42 (5), 901–910.

Sunda, W.G., Swift, D.G., Huntsman, S.A., 1991. Low iron requirement for growth in oceanic phytoplankton. Nature 351 (6321), 55–57.

Sunda, W.G., 2001. Bioavailability and bioaccumulation of iron in the Sea. In: Turner, D.R., Hunter, K.A. (Eds.), The Biogeochemistry of Iron in Seawater, vol. 7. Wiley & Sons, pp. 41–84 (Chapter 3).

Thuróczy, C.-E., Gerringa, L.J.A., Klunder, M.B., Middag, R., Laan, P., Timmermans, K.R., de Baar, H.J.W., 2010. Speciation of Fe in the Eastern North Atlantic Ocean. Deep-Sea Research I 57 (11), 1444–1453.

Timmermans, K.R., Gledhill, M., Nolting, R.F., Veldhuis, M.J.W., de Baar, H.J.W., van den Berg, C.M.G., 1998. Responses of marine phytoplankton in iron enrichment experiments in the northern North Sea and northeast Atlantic Ocean. Marine Chemistry 61 (3–4), 229–242.

Timmermans, K.R., Davey, M.S., van der Wagt, B., Snoek, J., Geider, R.J., Veldhuis, M.J.W., Gerringa, L.J.A., de Baar, H.J.W., 2001. Co-limitation by iron and light of *Chaetoceros brevis*, *C. dichaeta* and *C. calcitrans* Bacillariophyceae. Marine Ecology Progress Series 217, 287–297.

Timmermans, K.R., van der Wagt, B., de Baar, H.J.W., 2004. Growth rates, half-saturation constants, and silicate, nitrate, and phosphate depletion in relation to iron availability of four large, open-ocean diatoms from the Southern Ocean. Limnology and Oceanography 49 (6), 2141–2151.

Tortell, P.D., Maldonado, M.T., Price, N.M., 1996. The role of heterotrophic bacteria in iron-limited ocean ecosystems. Nature 383 (6598), 330–332.

Tortell, P.D., Maldonado, M.T., Granger, J., Price, N.M., 1999. Marine bacteria and biogeochemical cycling of iron in the oceans. FEMS Microbiology and Ecology 29 (1), 1–11.

Turoczy, N.J., Sherwood, J.E., 1997. Modification of the van den Berg/Ruzic method for the investigation of complexation parameters of natural waters. Analytica Chimica Acta 354 (1–3), 15–21.

Wells, M.L., Goldberg, E.D., 1993. Colloid aggregation in seawater. Marine Chemistry 41 (4), 353–358.

Wells, M.L., Goldberg, E.D., 1994. The distribution of colloids in the North Atlantic and Southern Oceans. Limnology and Oceanography 39 (2), 286–302.

Wells, M.L., Smith, G.J., Bruland, K.W., 2000. The distribution of colloidal and particulate bioactive metals in Narragansett Bay, RI. Marine Chemistry 71 (1–2), 143–163.

Witter, A.E., Luther III., G.W., 1998. Variation in Fe–organic complexation with depth in the Northwestern Atlantic Ocean as determined using a kinetic approach. Marine Chemistry 62 (3–4), 241–258.

Wu, J., Luther III., G.W., 1995. Complexation of Fe(III) by natural organic ligands in the Northwest Atlantic Ocean by a competitive ligand equilibration method and a kinetic approach. Marine Chemistry 50 (1–4), 159–177.

Wu, J., Boyle, E., Sunda, W., Wen, L.-S., 2001. Soluble and colloidal iron in the oligotrophic north Atlantic and north Pacific. Science 293 (5531), 847–849.